Early onset combined immunodeficiency and autoimmunity in patients with loss-of-function mutation in *LAT*

Baerbel Keller,[1]* Irina Zaidman,[2]* O. Sascha Yousefi,[1,3,4]* Dov Hershkovitz,[5] Jerry Stein,[6] Susanne Unger,[1] Kristina Schachtrup,[1] Mikael Sigvardsson,[7] Amir A. Kuperman,[8,9] Avraham Shaag,[10] Wolfgang W. Schamel,[1,3]** Orly Elpeleg,[10]** Klaus Warnatz,[1]** and Polina Stepensky[10,11]**

[1]Center for Chronic Immunodeficiency (CCI), University Medical Center and University of Freiburg, 79106 Freiburg, Germany
[2]Department of Pediatric Hematology Oncology, Ruth Rappaport Children's Hospital, Rambam Health Care Campus, Haifa 3109601, Israel
[3]Department of Molecular Immunology, Faculty of Biology, BIOSS Centre for Biological Signalling Studies, University of Freiburg, 79104 Freiburg, Germany
[4]Spemann Graduate School of Biology and Medicine (SGBM), Albert Ludwigs University Freiburg, 79104 Freiburg, Germany
[5]Department of Pathology, Rambam Health Care Campus, Haifa 3109601, Israel
[6]Department of Pediatric Hematology Oncology and Bone Marrow Transplantation Unit, Schneider Children's Medical Center of Israel, Petah-Tikva 49202, Israel
[7]Department of Clinical and Experimental Medicine, Experimental Hematopoiesis Unit, Faculty of Health Sciences, Linköping University, 581 85 Linköping, Sweden
[8]Blood Coagulation Service and Pediatric Hematology Clinic, Galilee Medical Center, Nahariya 22100, Israel
[9]Faculty of Medicine in the Galilee, Bar-Ilan University, Safed 5290002, Israel
[10]Monique and Jacques Roboh Department of Genetic Research and [11]Department of Pediatric Hematology-Oncology and Bone Marrow Transplantation, Hadassah Medical Center, Hebrew University, Jerusalem 91120, Israel

The adapter protein linker for activation of T cells (LAT) is a critical signaling hub connecting T cell antigen receptor triggering to downstream T cell responses. In this study, we describe the first kindred with defective LAT signaling caused by a homozygous mutation in exon 5, leading to a premature stop codon deleting most of the cytoplasmic tail of LAT, including the critical tyrosine residues for signal propagation. The three patients presented from early childhood with combined immunodeficiency and severe autoimmune disease. Unlike in the mouse counterpart, reduced numbers of T cells were present in the patients. Despite the reported nonredundant role of LAT in Ca^{2+} mobilization, residual T cells were able to induce Ca^{2+} influx and nuclear factor (NF) κB signaling, whereas extracellular signal–regulated kinase (ERK) signaling was completely abolished. This is the first report of a LAT-related disease in humans, manifesting by a progressive combined immune deficiency with severe autoimmune disease.

T cells are selected during thymic development based on the signal strength elicited through the interaction of the MHC–peptide complex on APCs and the TCR on thymocytes. Although the specificity of the TCR plays a crucial role and allows for positive and negative selection, amplifying or dampening alterations of signaling proteins downstream of the TCR will modify signal strength and, consequently, impact the cellular response and outcome of selection. Multiple examples have illustrated the effect of altered TCR signal strength on the increased survival of autoreactive T cell clones in mice with genetic alterations of signaling molecules like ZAP70 (Sakaguchi et al., 2003; Siggs et al., 2007) or the CD3 signaling unit by deletion of several immunoreceptor tyrosine-based activating motives (Holst et al., 2008). This signaling machinery downstream of the TCR is composed of a dynamic, fine-tuned network of multiple components that interact in a tightly regulated temporospatial manner. This is achieved by scaffold proteins, which allow the preassembly of signalosomes to facilitate rapid signal transduction and guarantee signal specificity. Although the lack of certain scaffold proteins like BLNK/SLP65 in B cells (Minegishi et al., 1999) leads to the absence of affected lymphocyte subsets, the lack of others may allow for the development of the respective population but modify their activation or further differentiation.

Linker for activation of T cells (LAT) is a transmembrane adapter molecule first discovered in activated T cells. LAT is phosphorylated after TCR triggering at four conserved tyrosine residues that are essential for the recruitment and membrane localization of downstream molecules: human (h)Y132/mouse (m)Y136, hY171/mY175, hY191/mY195, and hY226/mY235 (Balagopalan et al., 2010). LAT knockout mice (Zhang et al., 1999b) and mice with targeted replacement of all four tyrosine residues (Sommers et al., 2001) lack peripheral T cells because of a block at the double-negative 3 stage. These tyrosines serve as docking

*B. Keller, I. Zaidman, and O.S. Yousefi contributed equally to this paper.

**W.W. Schamel, O. Elpeleg, K. Warnatz, and P. Stepensky contributed equally to this paper.

Correspondence to Klaus Warnatz: klaus.warnatz@uniklinik-freiburg.de; or Polina Stepensky: polina@hadassah.org.il

Abbreviations used: DAG, diacylglycerol; DGK, DAG kinase; ERK, extracellular signal-regulated kinase; ICOS, inducible T cell co-stimulator; IP_3, inositol 1,4,5-trisphosphate; ITK, IL-2–inducible T cell kinase; LAB, linker for activation of B cells; LAT, linker for activation of T cells; NTAL, non–T cell activation linker.

The Rockefeller University Press $30.00
J. Exp. Med. 2016 Vol. 213 No. 7 1185–1199
www.jem.org/cgi/doi/10.1084/jem.20151110

The Journal of Experimental Medicine

sites for PLCγ1, Grb2, Gads, and others, interconnected in positive and negative regulatory plug-ins of (pre)assembled signaling modules (Malissen et al., 2014; Roncagalli et al., 2014) modifying T cell development (Zhang et al., 1999b), specific functions (Ou-Yang et al., 2012), or even terminating T cell activation (Malissen et al., 2014). Mice with a mutation at Y136 of LAT, which is the docking site for PLCγ1, present with hypergammaglobulinemia and severe lupus-like glomerulonephritis and die within 6 wk (Sommers et al., 2002), suggesting an essential role of this docking site for negative regulatory plug-ins. This deletion uncouples the activation of the CD28 pathway from the TCR by allowing for TCR-independent constitutive activation. Because of the distinctive pattern of this dysregulation in affected mice, it was termed LAT signaling pathology (Roncagalli et al., 2010). In contrast to mice, the physiological role of LAT is not known in humans.

Here, we describe for the first time the clinical course and immunological findings in a family with a homozygous loss-of-function mutation in LAT.

RESULTS

Case studies

We evaluated three siblings born to consanguineous parents of Arab origin (Fig. 1). All three patients presented with recurrent infection, lymphoproliferation, and life-threatening autoimmune disease since early infancy. The main clinical and laboratory findings are summarized in Table 1.

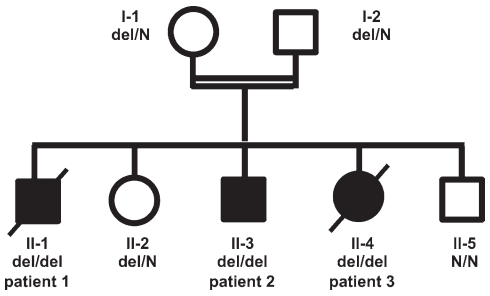

Figure 1. **Pedigree of the affected family.** Circles represent female and squares represent male subjects. Solid symbols show homozygous affected patients, and crossed-out symbols stand for deceased subjects. N, wild type. del, deletion.

Patient 1 presented at the age of 5 mo with the first severe episode of Coombs-positive autoimmune hemolytic anemia and immune-mediated thrombocytopenia, lymphadenopathy, and massive splenomegaly. For progressive treatment–resistant autoimmune cytopenia, he was splenectomized at the age of 7 yr, but at age 9, awaiting hematopoietic stem cell transplan-

Table 1. **Summary of major clinical and laboratory findings**

	Patient 1, male	Patient 2, male	Patient 3, female
Age at presentation	5 mo	6 mo	10 mo
Infection	Recurrent pneumonia, EBV/CMV viremia, CMV pneumonia	Congenital toxoplasmosis, recurrent pneumonia, varicella infection, CMV viremia, Candida pneumonia adenovirus + CMV PCR positive in BAL	Recurrent pneumonia, urinary infections, gastroenteritis, CMV viremia
Autoimmunity	Coombs$^+$ AIHA, ITP, autoimmune neutropenia	Coombs$^+$ AIHA, ITP	Anti-ADAMTS13$^+$ microangiopathic hemolytic anemia
Lymphoproliferation	Lymphadenopathy, splenomegaly	Lymphadenopathy, splenomegaly	Lymphadenopathy, splenomegaly
Lung disease	Chronic lung disease, bronchiectasis	Chronic lung disease, bronchiectasis	No
Others	Red-brown rash on face and legs	Diplegic cerebral palsy due to congenital toxoplasmosis, red-brown rash on forearm	No
Treatment	Steroids, IgG-RT, splenectomy	Steroids, IgG-RT	Steroids, plasmapheresis
Outcome	Died at 9 yr due to disseminated CMV infection	Alive, 8 yr old, 13 mo after HSCT	Died at 2 yr due to TTP
Immunoglobulins	Progressive hypogammaglobulinemia <4 yr: normal 4 yr: IgG 1.6 g/liter (5.4–13.4 g/liter) IgA <0.16 g/liter (0.3–1.9 g/liter) IgM 0.12 g/liter (0.4–1.7 g/liter) IgE 2 IU/ml (<58 IU/ml)	Progressive hypogammaglobulinemia <3.5 yr: normal to rather increased 3.5 yr: IgG 1.3 g/liter (5.4–13.4 g/liter) IgA 0.69 g/liter (0.3–1.9 g/liter) IgM 0.84 g/liter (0.4–1.7 g/liter) 8 yr: IgG <2 g/liter (6.5–15.3 g/liter) IgA <0.26 g/liter (0.5–2.5 g/liter) IgM 0.39 g/liter (0.4–1.9 g/liter)	Hypergammaglobulinemia 2 yr: IgG 20.45 g/liter (4.7–12.3 g/liter) IgA 1.02 g/liter (0.2–1.4 g/liter) IgM 0.89 g/liter (0.4–1.5 g/liter) IgE 286 IU/ml (<29 IU/ml)
Specific antibodies	Hepatitis A$^+$, HSV1$^+$, Hepatitis B$^-$, measles$^-$, mumps$^-$, rubella$^-$	ND	rubella$^+$, measles$^-$, EBV$^+$, CMV$^-$
Lymphocyte populations	Progressive lymphopenia, high γδ T cells, low CD4 T cells	Progressive lymphopenia, high γδ T cells, low CD4 T cells, low B cells	High γδ T cells

AIHA, autoimmune hemolytic anemia; BAL, bronchoalveolar lavage; HSCT, hematopoietic stem cell transplantation; IgG-RT, Ig replacement therapy; ITP, idiopathic thrombocytopenic purpura; TTP, thrombotic thrombocytopenic purpura. Values in parentheses depict age-matched reference values.

tation, he died because of disseminated CMV infection with pulmonary involvement. He had additionally suffered from chronic lung disease with bronchiectasis and disseminated purple edematous skin lesions on his face and arms.

The index patient (patient 2) presented at the age of 7 mo with diplegic cerebral palsy and megalocystic leukencephalopathy probably caused by perinatal toxoplasmosis infection. From 1 yr of age, he suffered from recurrent respiratory tract infections, which progressed to chronic lung disease with bronchiectasis. Like his brother, he suffered from hepatosplenomegaly, lymphadenopathy, and persistent red edematous nodules on his forearms. From the age of 6 yr, he was treated with steroids for severe Evans syndrome. At age 7 yr, varicella infection was diagnosed, and shortly after, he developed CMV and adenoviral infection with severe progressive deterioration of respiratory function. On antiviral and IgG replacement therapy, he improved gradually, and genetic diagnosis was performed. Currently, at the age of 8 yr, he successfully received an allogeneic stem cell transplantation from his fully matched heterozygous sibling.

The younger sister (patient 3) presented at the age of 10 mo with gastroenteritis, recurrent pneumonia, and urinary tract infection. At the age of 2 yr, she died of anti -ADAMTS13–positive microangiopathic hemolytic anemia and thrombocytopenia.

The histological examination of lymph nodes from patients 1 and 2 showed distorted architecture with poorly formed follicles (not depicted). Aggregates of small, CD20-positive cells were associated with CD21-positive follicular dendritic cells, but Bcl6-positive germinal centers were absent. The spleen of patient 1 resembled the findings in the lymph nodes (not depicted). The skin biopsies showed extensive lymphoid infiltration of the dermis but not the epidermis, mainly by CD8 T cells. In situ hybridization for EBV-encoded RNA in the skin was negative as well as histochemical stains for fungi and acid-fast bacteria (not depicted).

Immune phenotype of LAT-mutated patients

Patient 1 presented with initially normal T, B, and NK cell counts, mitogen responses (Con A and pokeweed mitogen), and serum Ig levels. At the age of 4 yr, he developed hypogammaglobulinemia with partially reduced specific antibody responses. An increased number of γδ T cells (up to 80% of T cells) was noted on several occasions. At 6 yr of age, decreased CD4 T cells and B cells and increased CD4-negative/CD8-negative T cells, presumably representing the already beforehand increased γδ T cells (Table 2), were noted.

Patient 2 showed repeatedly normal numbers of T, B, and NK cells. Ig levels dropped from hypergammaglobulinemia with normal IgA and IgM to panhypogammaglobulinemia. At the age of 8, IgG replacement therapy was started. T, B, and NK cells gradually decreased from the age of 6 yr with persistently increased numbers of γδ T cells. At the age of 8 yr, patient 2 had developed panlymphopenia leading to strongly reduced absolute counts of all B and CD4 T cell subpopulations. CD4 T cells were severely decreased, especially affecting the naive CD4 T cell subpopulation, whereas the percentage of regulatory T cells and circulating T follicular helper cell populations showed minor changes (Table 2). Comparing the distribution of CCR7, CD27, and CD28 (Okada et al., 2008) in CD45R0 CD4 T cells of the patient with five healthy controls, we observed a relative increase of ($CCR7^-$/$CD27^+$/$CD28^+$) effector memory T cells (33.4%; mean ± standard deviation, 23.2 ± 7.4%), reduced ($CCR7^+$/$CD27^+$/$CD28^+$) central memory T cells (3.5%; 13.3 ± 4.9%), and a relative increase of ($CCR7^-$/$CD27^-$/$CD28^{+/-}$) effector T cells (42.6%; 8.1 ± 6.5%), which is even more remarkable given the young age of the patient. Among CD8 T cells, naive and terminally differentiated CD8 T cells were diminished, but central and effector memory CD8 T cells were normal. Absolute and relative numbers of B cells were reduced, and a relative increase of transitional B cells was observed, whereas class-switched and IgM memory B cells were strongly decreased. Given the initial records of normal numbers of B and NK cells in patient 2 and normal Ig levels in all siblings at a younger age, the latter changes are likely to be secondary to progressive immune dysregulation.

The immunological evaluation of patient 3 at the age of 2 yr was remarkable for hypergammaglobulinemia and elevated IgE. She had reduced NK cells but normal numbers of B cells and total T cells. The T cell compartment showed reduced relative and absolute CD4 T cells and reduced percentages of CD8 T cells but, like her siblings, strongly increased γδ T cells (Table 2).

In the heterozygous parents, all lymphocyte subset counts and Ig levels were within the normal range, whereas the heterozygous sister had nearly 10% γδ T cells and slightly increased levels of all Ig isotypes (unpublished data).

Molecular characterization of the LAT mutation

The exome analysis of patient 2 yielded 54.1 million confidently mapped reads with a mean coverage of ×62. After alignment to the reference genome (Hg19) and variant calling, we removed variants that were called less than ×8, were off target, synonymous, heterozygous, predicted benign by Mutation Taster software, with minor allele frequencies >0.1% in the dbSNP138 or minor allele frequencies >1% in the Hadassah in-house database. 12 homozygous variants remained, but only chr16:28997725 deletion (del) GG (RefSeq accession no. NM_001014987.1: c.268_269del) segregated with the disease in the family. The mutation was not present in any of the nearly 60,000 exomes deposited by the Exome Aggregation Consortium. This mutation caused a deletion of guanosines 268/269 in exon 5 of *LAT*, leading to a frame shift and a premature stop codon after 303 bp (Fig. 2 A). The predicted protein of 100 of the 233 aa contains an intact extracellular and transmembrane region but a shortened intracellular region, eliminating the known major phosphorylation sites Y132, Y171, Y191, and Y226 (Fig. 2 B). We did not identify any additional pathogenic mutations by whole exome sequencing.

The relative amount of *LAT* mRNA in patient's sorted CD4 CD45R0 T cells was within the range of three different healthy controls (Fig. 2 C), indicating that the mutation does not interfere with transcript stability. The LAT protein, however, could not be detected by flow cytometry using an antibody directed against the intracytoplasmic part of LAT in CD4 T cells (Fig. 2 D) and by Western blotting of patient-derived EBV lines using a polyclonal antibody against LAT (not depicted). Interestingly, LAT staining in the heterozygous sibling showed normal levels of LAT in the majority of cells but a small percentage of cells with low to absent protein expression (Fig. 2 D). To test whether the putative truncated protein can be expressed, LAT-deficient Jurkat-derived J.CaM2.5 cells (Finco et al., 1998) were stably transduced with the mutated form of the protein (J.CaM2.5-LAT^{mut}) or with wild-type LAT (J.CaM2.5-LAT^{wt}). Both were tagged with a FLAG sequence and cotransfected with ZsGreen1 separated by an internal ribosomal entry site. FLAG expression correlated with ZsGreen1 expression, indicating that translation efficiency of the FLAG-tagged LAT and the ZsGreen1 sequence is identical (Fig. 2 E). Western blotting with anti-FLAG tag but not the polyclonal anti-LAT antibody (not depicted) detected a shortened LAT^{mut} protein in the transduced J.CaM2.5-LAT^{mut} cells compared with J.CaM2.5-LAT^{wt} cells (Fig. 2 F), indicating that the mutated LAT protein can be expressed. The loss of dominant immunogenic epitopes in the truncated LAT might explain the absent recognition by the polyclonal antibody targeting full-length LAT.

Signaling capacity of mutant LAT in Jurkat cells

The TCR-induced LAT signaling capacity was analyzed in J.CaM2.5-LAT^{wt} or J.CaM2.5-LAT^{mut} cells. After CD3

Table 2. **Immune phenotype of patient 1, 2, and 3**

	Patient 1 (6 yr)				Patient 2 (8 yr)				Patient 3 (2 yr)			
	Relative counts	Reference values	Absolute	Reference values	Relative counts	Reference values	Absolute	Reference values	Relative counts	Reference values	Absolute	Reference values
Lymphocytes[a]			1,855	1,800–5,000			900	1,800–5,000			4,950	2,800–6,400
B cells[a]	2.0	8.5–20.2	37	296–784	3.8	8.5–20.2	34	296–784	29.9	17.3–30.0	1,480	686–1,732
CD4[a]	4.0	26.5–41.4	74	641–1,453	24.5	26.5–41.4	220	641–1,453	6.4	28.1–43.2	317	925–2,477
CD8[b]	45.0	13–47	834	200–1,700	38.3	13–47	345	200–1,700	4.5	9–49	223	200–1,800
NK cells[b]	6.0	2–31	114	70–590	1.7	2–31	16	70–590	0.9	2–25	45	61–510
B cell subpopulations[a]	ND		ND						ND		ND	
Transitional					21.1	3.4–9.0	5	13–63				
Naive					68.7	47.8–69.8	23	154–413				
IgM memory					3.5	6.3–22	2	24–135				
IgM only					0.7	2–11.8	1	7–65				
IgA cs memory					0	1.1–6.1	0	5–35				
IgG cs memory					0	2.7–14	0	13–74				
CD21^{low}					6.3							
CD4 subpopulations[a]	ND		ND						ND		ND	
RTE[c]					24.4	61–84.2	1					
Naive					2.4	55.6–75.8	5	375–1,096				
CD45R0					97.5	24–43						
T reg cells					2.0	2.3–7.7	5	18–86				
cTFH[d]					35.0	18.4–29.9	112	51–218				
$Th_2^+Th_{17}$-like cTFH[d]					29.4	39.9–66.1	33	26–85				
CD8 subpopulations[b]	ND		ND						ND		ND	
Naive					0.3	16–100	1	42–1,300				
Central memory					2.4	1–6	8	6–43				
Effector memory					65.9	5–100	227	45–410				
Terminally differentiated					1.6	15–41	6	57–340				
γδ T cells[e]	ND		ND		37.2	<10	282	12–175	72	<10	2,217	12–175
DN T cells[e]	51				38				72			
NK T cells[e]	ND		ND		0.005	>0.01	ND		ND		ND	

Relative counts are shown as a percentage of parental population. Absolute numbers refer to cells/microliter. CD4 T cell subpopulations: recent thymic emigrants (RTEs), CD31$^+$ of CD45RA$^+$ CD4 T cells; T reg cells, CD127$^-$ CD25hi of CD45RA$^-$ CD4 T cells; circulating T follicular helper–like cell (cTFH), CXCR5$^+$ of CD45RA$^-$ CD4 T cells; Th2/Th17-like cTFH, CXCR3$^-$ of CXCR5$^+$ CD45RA$^-$ CD4 T cells. CD8 T cell populations: naive, CCR7$^+$ CD45RA$^+$ CD27$^+$; terminally differentiated, CCR7$^-$ CD45RA$^+$ CD27$^-$; central memory, CCR7$^+$ CD45RA$^-$ CD27$^+$; effector memory, CCR7$^-$ CD45RA$^-$ CD27$^-$. Double-negative (DN) T cells, CD4$^-$/CD8$^-$ of CD3 T cells. NK T cells, Vα24 Vβ11 CD3 T cells. cs, class switched.

[a]van Gent et al., 2009.

[b]Schatorjé et al., 2012.

[c]Percentage of naive CD4 T cells.

[d]Internal reference value.

[e]Internal reference value of CD3 T cells.

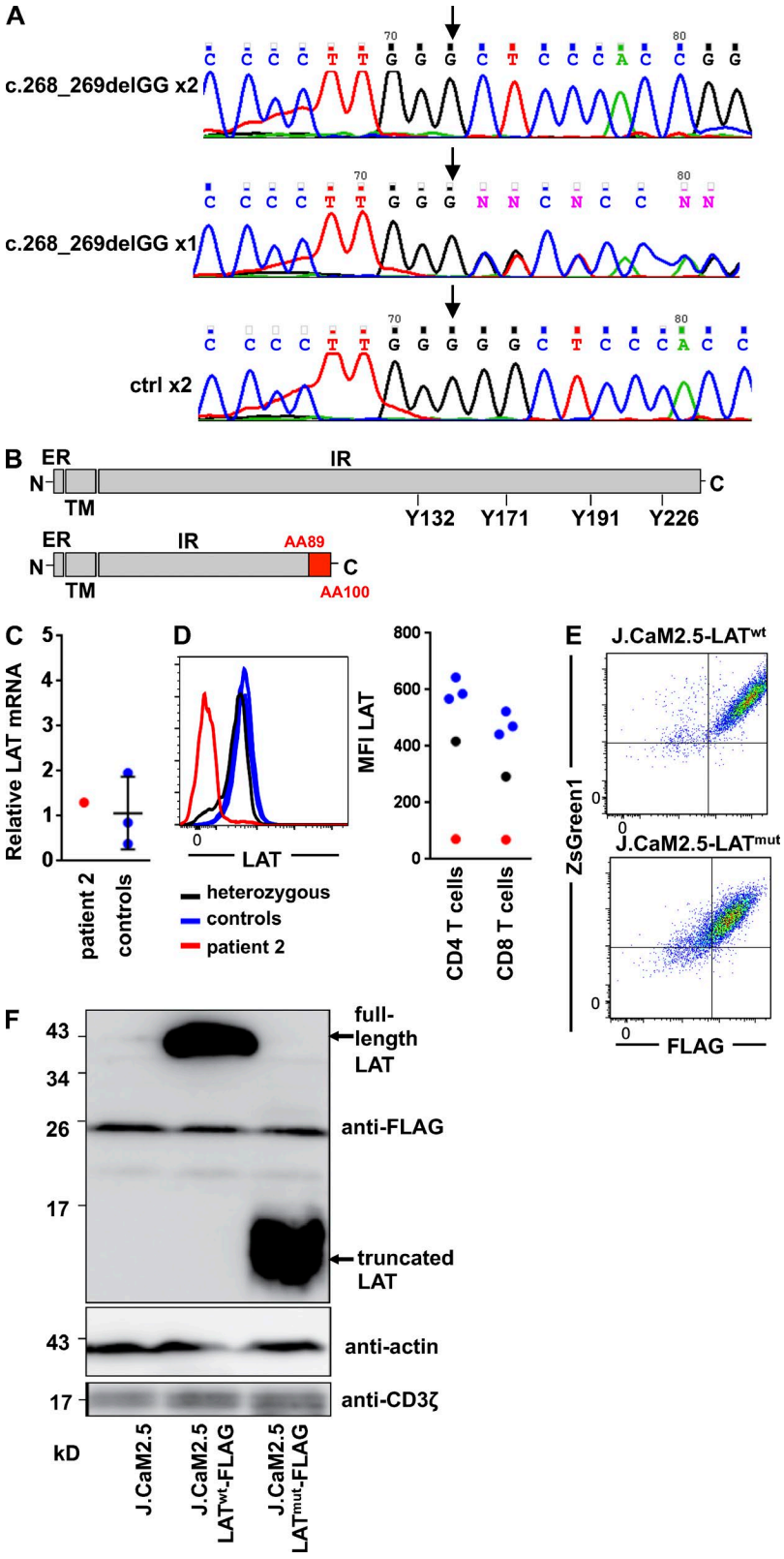

Figure 2. **Molecular characterization of LAT mutation.** (A) Genomic DNA sequence around the c.268_269delGG mutation site (arrows) of a patient (top), a parent (middle), and an unrelated healthy control (ctrl; bottom). (B) Schematic view of wild-type LAT showing the extracellular region (ER), the transmembrane domain (TM), and the intracellular region (IR) with the four tyrosine residues phosphorylated downstream of TCR signaling. Below is the mutated form of the protein. The presumptive position of the frame shift starting at 89 aa and the presumed truncation after 100 aa is shown in red. (C) Relative mRNA expression of LAT with hypoxanthine phosphoribosyltransferase as the housekeeping gene is shown in CD4 CD45RO T cells of patient 2 and three controls normalized to Jurkat cells. (D) FACS plot for LAT expression gated on CD4 CD45RO T cells and graph of the mean fluorescence intensity (MFI) of LAT in CD4 and CD8 T cells in patient 2, the heterozygous sister, and three healthy controls. (E) Anti-FLAG staining and ZsGreen1 expression are shown in J.CaM2.5 cells expressing the recombinant wild-type (LAT^{wt}) or the mutated LAT protein (LAT^{mut}). (F) Immunodetection of FLAG-tagged LAT^{wt} or LAT^{mut} in J.CaM2.5 cells. The immunoblot is representative of three independent experiments.

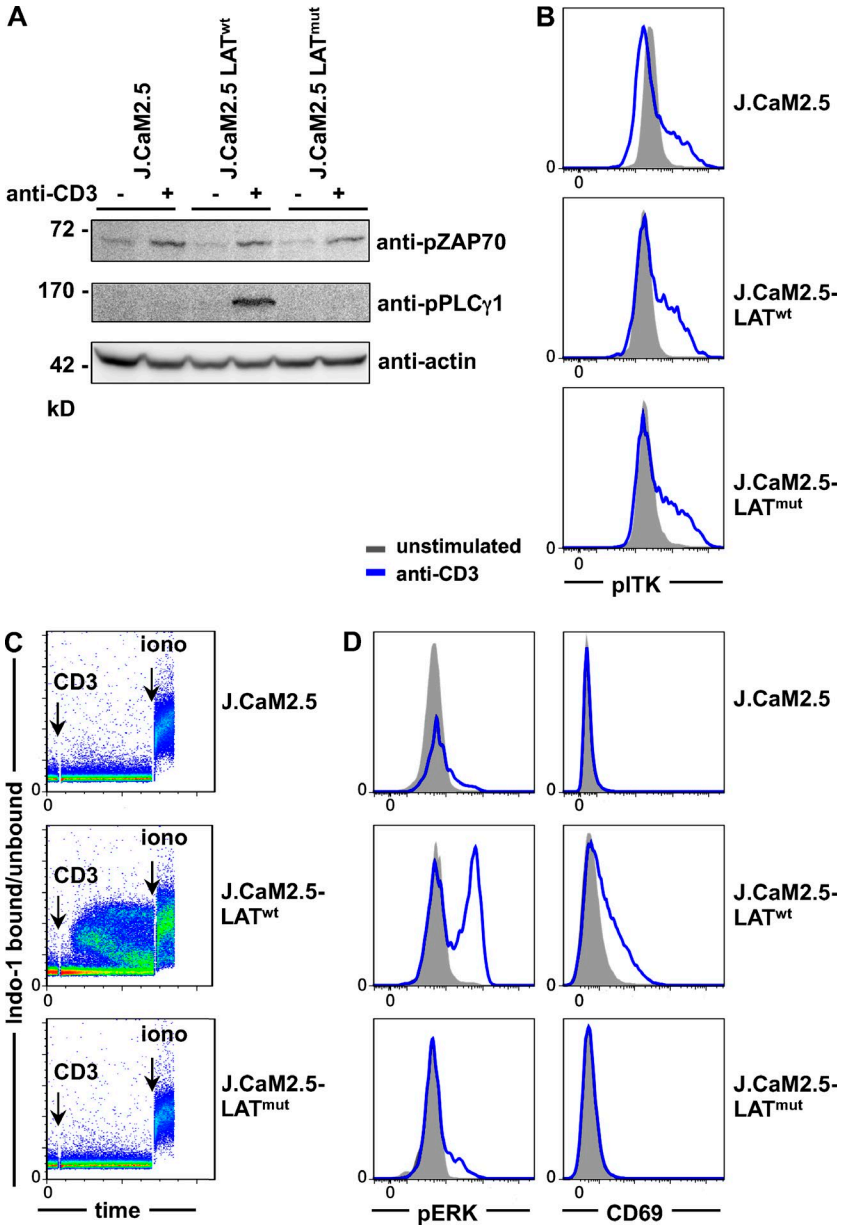

Figure 3. **TCR-induced signaling in LAT^{mut} T cells.** (A–D) All experiments were performed in LAT-deficient J.CaM2.5 cells and J.CaM2.5 cells reconstituted with LAT^{wt} or LAT^{mut}. (A) Immunoblot of ZAP70 and PLCγ1 phosphorylation with or without stimulation with 5 µg/ml anti-CD3 for 3 min. (B) Phosphorylation of ITK (pITK) with or without stimulation with 5 µg/ml anti-CD3 for 2 min. (C) Ca^{2+} mobilization after anti-CD3 stimulation. (D) Phosphorylation of ERK (pERK) after 2-min anti-CD3 stimulation and up-regulation of CD69 after overnight stimulation. All results are representative of three to five independent experiments.

cross-linking, similar TCR-proximal ZAP70 phosphorylation was observed in LAT-deficient, LAT^{wt}-, and LAT^{mut}-expressing T cell lines (Fig. 3 A). In line with the literature that PLCγ1 phosphorylation depends on the assembly of the LAT-SLP76 signalosome (Smith-Garvin et al., 2009), PLCγ1 phosphorylation was absent in J.CaM2.5 and J.CaM2.5-LAT^{mut} cells (Fig. 3 A). Interestingly, the phosphorylation of IL-2–inducible T cell kinase (ITK), also reported to be dependent on LAT (Shan and Wange, 1999), was not affected by the absence of LAT or the presence of LAT^{mut} (Fig. 3 B). TCR-induced Ca^{2+} mobilization was restored by LAT^{wt} expression but absent in J.CaM2.5 and J.CaM2.5-LAT^{mut} cells (Fig. 3 C), indicating that the truncated protein itself is not capable of mediating TCR-induced inositol 1,4,5-trisphosphate (IP_3) production and subsequent Ca^{2+} flux. Similarly, extracellular signal-regulated kinase (ERK) phosphorylation and up-regulation of CD69 was strongly reduced in J.CaM2.5-LAT^{mut} and J.CaM2.5 cells compared with J.CaM2.5-LAT^{wt} cells (Fig. 3 D), showing that the mutation interferes with LAT signaling.

Signaling in LAT^{mut} lymphocytes

Next, we addressed the effect of the mutated LAT on TCR signaling in primary T cells of patient 2 after stimulation with anti-CD3 or anti-CD3/anti-CD28. As previously reported in LAT-deficient mice (Archambaud et al., 2009), we observed significantly decreased CD3 expression on LAT^{mut} CD4 T cells (Fig. 4 A), in contrast to mice not on CD8 T cells.

In line with reconstituted J.CaM2.5 cells, phosphorylation of ITK was observed in CD45R0 CD4 T cells of patient 2 after CD3 cross-linking (Fig. 4 B), and the phosphorylation of ERK was absent in LAT^{mut}-expressing CD4 T cell subpopulations (Fig. 4 C). Surprisingly, and in contrast to our reconstitution experiments and to mouse LAT-deficient T cells, Ca^{2+} mobilization was detectable in three independent experiments in CD45R0 CD4 T cells and CD45R0 CD8 T cells of the patient and was predominantly within the range of healthy controls (Fig. 4 D). Ca^{2+} mobilization in naive CD4 was not evaluable because of extremely low cell counts. In line with the preserved Ca^{2+} response, IκBα degradation, which is also downstream of PLCγ1 activation, occurred normally after CD3/CD28 co-stimulation (Fig. 4 E), indicating that signaling was partially maintained in primary T cells in the absence of LAT. Genomic DNA sequencing of isolated CD45R0 CD4 T cells was performed to exclude reversion of the mutation as a potential explanation for this finding. However, only mutated *LAT* was detected in this population (not depicted). In addition, the possibility of alternative splicing was addressed by testing the mutant sequence for potential new splice sites. Two possible variants were predicted in silico. However, both variants were not detectable by PCR. Furthermore, RNA sequencing data of sorted CD45R0 CD4, CD8, and γδ T cells showed various fragments covering the genomically encoded 2-bp deletion, but no fragments compatible with the predicted aberrant splicing variants were detected (unpublished data). In T cells of the heterozygous parents and sister, the phosphorylation of ZAP70, ITK, ERK, and Ca^{2+} mobilization was found to be normal (not depicted), indicating that there is no dominant-negative effect of the mutation in the heterozygous situation.

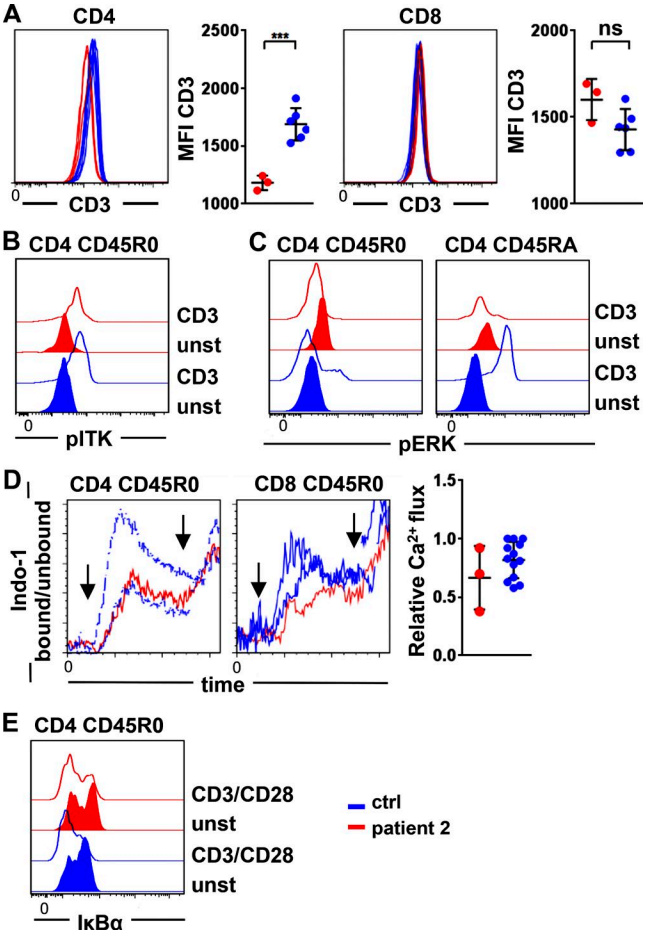

Figure 4. **TCR signaling in primary LAT-mutated T cells.** (A) Expression of CD3 on CD4 (left) and CD8 T cells (right) in three different experiments compared with controls. Patient 2 is shown in red, and controls are in blue. MFI, mean fluorescence intensity. ns, not significant. ***, $P \leq 0.001$. (B and C) Phosphorylation of ITK (pITK; B) and ERK (pERK; C) in patient's and controls' CD45RO and CD45RA CD4 T cells without (closed) and after CD3 stimulation (open). Results are representative of five and four independent experiments. (D) Ca^{2+} mobilization after cross-linking of CD3 is depicted in CD45RO CD4 T cells and CD45RO CD8 T cells of two controls and the LAT-mutated patient 2. Arrows indicate the addition of goat anti-mouse for CD3 cross-linking and ionomycin. The graph shows the relative Ca^{2+} influx determined by the peak of Indo-1 bound/unbound normalized to the highest day control in three independent experiments. (E) Degradation of IκBα is shown in CD45RO CD4 T cells of patient 2 and a healthy control after stimulation with anti-CD3/anti-CD28. Results are representative of two independent experiments. ctrl, control. unst, unstimulated.

Expression of alternative adapter molecules in LAT^{mut} T cells

Given the preserved Ca^{2+} response in primary T cells in contrast to J.CaM2.5-LAT^{mut} cells, we searched for adapter molecules potentially replacing the function of LAT with regard to Ca^{2+} mobilization. Expression of the adapter molecules SIT, TRIM (TCR-interacting molecule), LAX (linker for activation of X cells), LIME, and PAG did not remarkably differ in patients' T cells compared with two controls in RNA sequencing analysis (Fig. 5 A). Because RNA for non–T cell activation linker (NTAL)/linker for activation of B cells (LAB), the B cell homologue of LAT, was increased, we investigated protein expression in primary T cells but could not detect protein expression (Fig. 5 B).

CD6 was expressed on primary T cells of the patient and controls, whereas it was nearly absent on J.CaM2.5 cells (Fig. 5 C). To investigate the influence of CD6 on Ca^{2+} induction in the absence of LAT, J.CaM2.5, J.CaM2.5-LAT^{wt}, and J.CaM2.5-LAT^{mut} cells were stably transduced with CD6. Ca^{2+} mobilization was determined in nonselected CD6-transduced cell lines after gating on CD6-positive or CD6-negative cells. We could not observe an improvement of Ca^{2+} mobilization in CD6-expressing J.CaM2.5 and J.CaM2.5-LAT^{mut} cells, implying that CD6 could not compensate for LAT deficiency in these T cell lines (Fig. 5 D). Thus, CD6 expression in Jurkat-derived cell lines is not sufficient to replace LAT function.

Lymphocyte activation and function

The primary T cells of patient 2 were analyzed for functional impairment caused by the *LAT* mutation. In ac-

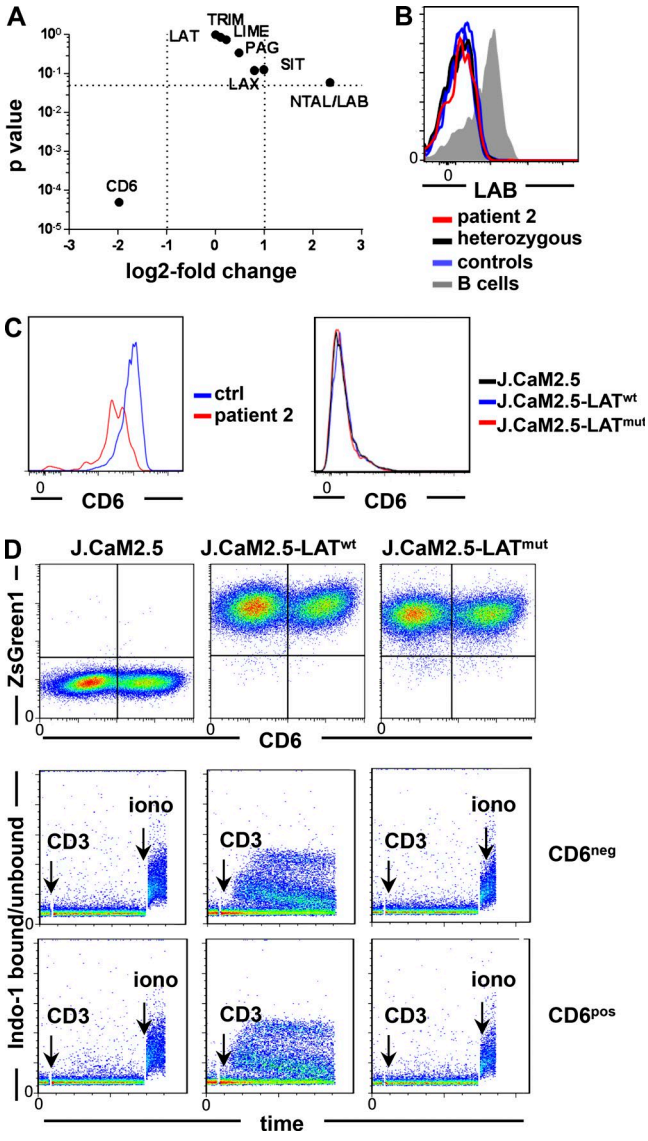

Figure 5. **Analysis of alternative adapter molecules in LAT-mutated T cells.** (A) Volcano plot displaying the p-value versus log2 fold change in gene expression of selected adapter molecules in CD4 CD45RO T cells of patient 2 compared with the mean expression value (base mean) of two controls determined by RNA sequencing. (B) Expression of LAB/NTAL in patient 2, the heterozygous sibling, and three controls. (C) CD6 expression in primary T cells of patient 2 and a healthy control (ctrl) and in LAT-transduced or nontransduced J.CaM2.5 cell lines (representative of two and four independent experiments, respectively). (D) CD6 and ZsGreen1 expression after transduction of a CD6 expression vector in J.CaM2.5, J.CaM2.5-LAT^{wt}, and J.CaM2.5-LAT^{mut} cells (top). Ca^{2+} mobilization in CD6-negative (CD6^{neg}) versus CD6-positive (CD6^{pos}) J.CaM2.5, J.CaM2.5-LAT^{wt}, and J.CaM2.5-LAT^{mut} cells after anti-CD3 stimulation (bottom). The results are representative of four independent experiments. iono, ionomycin.

cordance with LAT-deficient mice, a high percentage of LAT^{mut}-expressing CD4 T cells constitutively produced IL-4, implying an expansion of the T helper type 2 cell (Th2) phenotype (Fig. 6 A). In addition, the percentage of IFN-γ–producing CD4 T cells was slightly increased after PMA/ionomycin stimulation. The percentage of IL-17 and IL-2 producing CD45R0 CD4 T cells was similar to the controls after in vitro stimulation with PMA/ionomycin (Fig. 6 A). Anti-CD3 stimulation for 20 h induced only reduced levels of CD69, inducible T cell co-stimulator (ICOS), and CD25 in LAT^{mut} T cells, which could not be increased by the addition of anti-CD28 (Fig. 6 B). Similarly, in vitro proliferation of CD4 T cells (Fig. 6 C) and CD8 T cells (not depicted) after stimulation with anti-CD3, anti-CD3/anti-CD28 was abrogated and strongly reduced after PHA compared with the control. Finally, the degranulation of LAT^{mut} CTLs after stimulation with anti-CD3/anti-CD28 beads (Fig. 6 D) and of patient-derived NK cells after stimulation with the K562 cell line was reduced (Fig. 6 E), although not absent. Accordingly, NK cells of patient 1 showed diminished cytotoxicity compared with day controls (not depicted). This might reflect previous results from mice that signaling via LAT is not essential but beneficial for the process of degranulation (Ou-Yang et al., 2012; May et al., 2013).

CD4 T cells of the heterozygous parents and one heterozygous sibling displayed normal up-regulation of CD69, ICOS, and CD25 T cells, normal percentage of IFN-γ and IL-17–producing, but an increased percentage of IL-4–positive CD4 T cells in the 9-yr-old sibling (20%). NK cell degranulation in the heterozygous sibling was within the range of healthy controls (not depicted).

γδ T cells in LAT-mutated patient 2

A common finding in all patients was the remarkable increase of γδ T cells. γδ T cells of patient 2 consisted of 24% CD8^{dim} and 76% double-negative (CD4 negative/CD8 negative) γδ T cells, which is comparable to healthy controls. Unlike in healthy individuals, the most abundant circulating Vδ2-positive γδ T cell population was nearly absent in patient 2 (Fig. 7 A), and in line with this finding, Vγ9-positive cells were <5% (not depicted). 25% of the patient's γδ T cells expressed Vδ1, indicating that 74% Vδ1/Vδ2-negative γδ T cells expressed Vδ3, which could not be directly tested because of absent specific antibodies. Consistent with the findings in αβ T cells, Ca^{2+} mobilization was induced in γδ T cells after CD3 cross-linking and was comparable to healthy controls (Fig. 7 B).

As observed in healthy controls, most CD8-expressing γδ T cells produced IFN-γ upon PMA/ionomycin stimulation (not depicted). Among double-negative (CD4 negative/CD8 negative) γδ T cells, the number of spontaneous IL-4 producers was higher than in the controls, whereas IFN-γ–positive cell counts upon PMA/ionomycin stimulation were similar to healthy controls (Fig. 7 C), again showing the increase in the Th2 phenotype.

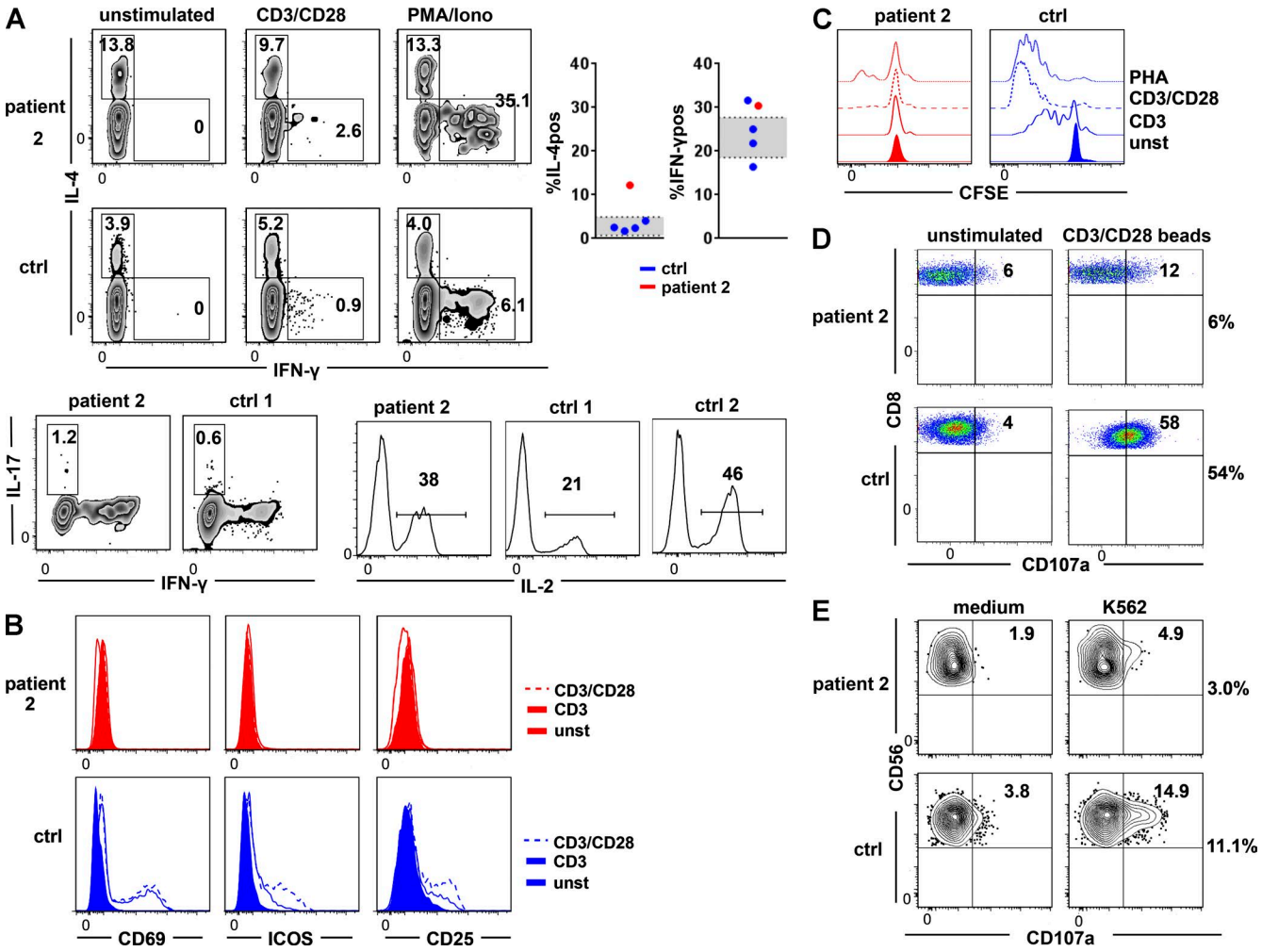

Figure 6. **Lymphocyte function.** (A) IL-4 and IFN-γ production in the unstimulated situation and after stimulation with PMA/ionomycin in the LAT-mutated patient and a control (top). The graphs show the percentage of IL-4– (IL-4pos) and IFN-γ–positive (IFN-γpos) cells of CD4 CD45RO T cells in patient 2 (red) compared with healthy day controls (blue). The standard deviation of 58 healthy controls is depicted in gray. IL-17 (bottom left) and IL-2 (bottom right) production after PMA/ionomycin (Iono) treatment in CD45RO CD4 T cells of patient 2 and one or two controls, respectively. Numbers indicate the percentage of positive cells in the respective parental subpopulation (three independent experiments). (B) Up-regulation of CD69, ICOS, and CD25 in the LAT-mutated patient (red) and a control (blue) after stimulation with anti-CD3 (continuous line) and anti-CD3/anti-CD28 (dashed line). Results are representative of two independent experiments. (C) Proliferation of CD4 T cells after stimulation with anti-CD3, anti-CD3/anti-CD28, and PHA (two independent experiments). unst, unstimulated. (D) CTL degranulation is shown by the up-regulation of CD107a in CD8 T cells after stimulation with CD3/CD28 beads. (E) NK cell degranulation measured by the surface expression of CD107a after incubation of PBMCs with K562 target cells (two independent experiments). ctrl, control.

DISCUSSION

Here, we describe the first kindred with a homozygous mutation in *LAT* presenting with a progressive combined immunodeficiency and profound immune dysregulation. All patients suffered from early onset autoimmune manifestations with normal lymphocyte counts and Ig levels. During the progression of the disease, the immune systems of the two older patients seemed to collapse, lymphocytopenia and hypogammaglobulinemia developed, and opportunistic as well as other infections occurred. The early death of patient 3 at 2 yr of age probably explains why she did not enter the second phase of the disease observed in her siblings. The mutation resulted in the expression of a truncated protein with a preserved extracellular and transmembrane region but lacking a large proportion of the intracellular adapter modules reported to be critically involved in TCR signaling pathways and T cell development in mice (Sommers et al., 2001).

LAT knockout mice (Zhang et al., 1999b) and mice with targeted replacement of all four tyrosine residues (Sommers et al., 2001) lack peripheral T cells because of a block at the double-negative 3 stage, whereas in humans, T cells lacking all four equivalent tyrosine residues were still present, although with a severely disturbed differentiation.

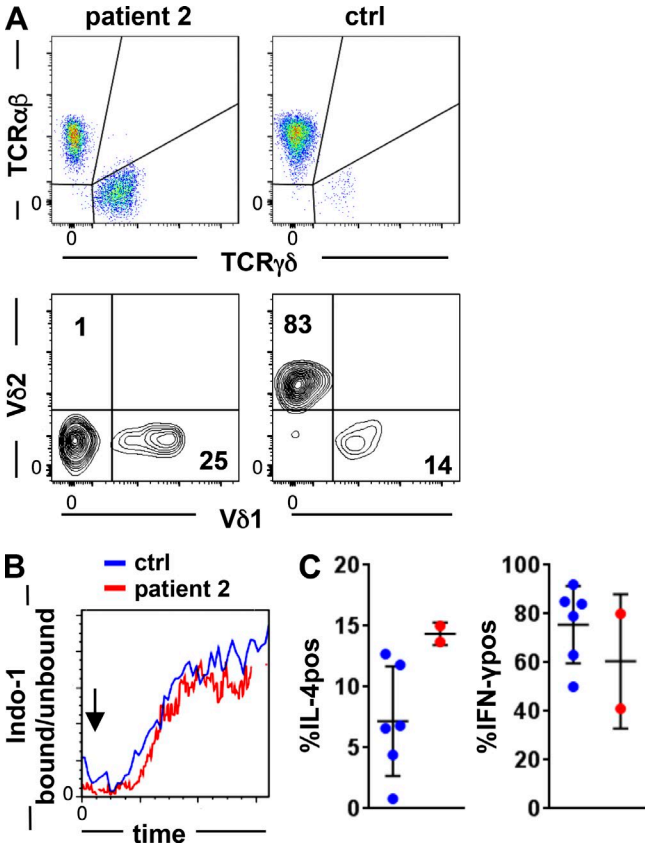

Figure 7. **γδ T cells in LAT mutation.** (A) FACS plots of γδ and αβ T cells in patient 2 and in a representative healthy control (top) and distribution of Vδ1 versus Vδ2 expression gated on γδ T cells (bottom). (B) Ca^{2+} mobilization in γδ T cells in the patient and a control. The arrow indicates the addition of goat anti-mouse for CD3 cross-linking. The experiment was performed once. (C) Percentage of spontaneous IL-4 producer (IL-4pos) and IFN-γ–positive (IFN-γpos) γδ T cells after PMA/ionomycin stimulation in two independent experiments compared with three healthy controls each. ctrl, control.

In mice, site-directed mutation of the PLCγ1 recruitment site Y136 caused a partial block in TCRαβ T cell differentiation, and over time, these mice developed a lymphoproliferative disorder, systemic autoimmunity, eosinophilia, and elevated IgE and IgG1 levels caused by a prominent Th2 cytokine shift (Aguado et al., 2002; Sommers et al., 2002). This is reminiscent of our patients with regard to lymphoproliferation, autoimmunity, and increased IL-4 production in αβ and γδ T cells of patient 2 (Aguado et al., 2002; Sommers et al., 2002; Genton et al., 2006). The association of a Th2 skewing and a weak TCR signaling has been observed in other mouse models (Corse et al., 2011) including an asthma model caused by low LAT-PLCγ1 interaction (Peng et al., 2014). Also, in humans with impaired TCR signaling strength, this association with Th2 has been described (Villa et al., 2008). In addition, effector T cells were generally expanded in the patient, including IFN-γ–producing T cells. An increased IFN-γ production upon stimulation compared with wild type has also been seen in the mouse LAT mutant models (Aguado et al., 2002; Sommers et al., 2002) and is probably an expression of the immune dysregulation and possibly infection in the patient. Mice with targeted mutations of the three distal tyrosine residues mY175, mY195, and mY235 developed an expansion of polyclonal γδ T cells in the spleen and in lymph nodes, reflecting the observation in the peripheral blood of our patients. However, in contrast to our LAT-deficient patients, in mice, the complete absence of LAT or the replacement of all four tyrosine residues of LAT abolished the emergence of γδ T cells in the periphery completely (Sommers et al., 2001; Nuñez-Cruz et al., 2003). The expanded γδ T cell population in the examined patient predominantly expressed Vδ3 and Vδ1 chains, whereas the common Vδ2 T cell compartment in healthy individuals (Xiong and Raulet, 2007) was absent. Interestingly, the expansion of Vδ3 T cells may contribute to the increased percentage of IL-4–producing γδ T cells (Mangan et al., 2013). A similar expansion of Vδ1 and Vδ3 T cells has been reported in CMV-seropositive patients after kidney and stem cell transplantation (Déchanet et al., 1999; Knight et al., 2010), and a potential involvement of these cells in the anti-CMV immune response has been implied. Of note, patient 2 had CMV viremia, possibly contributing to the skewed Vδ usage seen in this patient.

Thus, LAT-mutated mice and humans resemble each other with regard to severe immune dysregulation and lymphoproliferation associated with an expansion of γδ T cells and a disposition to a Th2 bias. Given the history of our patients, some of the differences compared with the mouse models like the emerging hypogammaglobulinemia and general lymphopenia might be secondary to infection and the increasing immune dysregulation, but the detectable development of mature T cells despite the absence of all four tyrosine signaling docking sites clearly demonstrates a difference between both species.

We therefore analyzed the signaling downstream of the TCR in detail after having excluded a genetic reversion of the *LAT* mutation and alternative splicing of the mRNA. In mouse T cells and human T cell lines, LAT has been demonstrated to be essential for Ca^{2+} mobilization and ERK phosphorylation after TCR stimulation (Lin and Weiss, 2001; Balagopalan et al., 2010). Thus, hY132/mY136 phosphorylation is required for the recruitment of PLCγ1, generation of IP_3, and subsequent Ca^{2+} mobilization in mouse T cells (Zhang et al., 2000). Consistent with this finding, the expression of LAT^{wt} but not LAT^{mut} protein in LAT-deficient J.CaM2.5 cells was able to rescue Ca^{2+} signaling. However, to our surprise, Ca^{2+} mobilization after CD3 cross-linking was normal in primary T cells of the index patient, and the sustained T cell differentiation in LAT-deficient patients supports the notion of a preserved residual TCR signal in vivo.

This discrepancy between human T cell lines and primary T cells might be caused by intrinsic differences in the signaling properties of cell lines and primary cells like the

absence of the phosphatases PTEN (phosphatase and tensin homolog) and SHIP-1 in Jurkat cells (Abraham and Weiss, 2004) or the presence of alternative transmembrane adapters replacing LAT function in primary T cells. SIT (Marie-Cardine et al., 1999), TRIM (Bruyns et al., 1998), LAX (Zhu et al., 2002), LIME (Brdičková et al., 2003; Hur et al., 2003), and PAG (Stepanek et al., 2014) share structural features with LAT but are expressed in both primary T cells and in Jurkat cells. Moreover, they were not differentially expressed in the primary cells of the index patient compared with controls on the RNA level, rendering the functional substitution for LAT unlikely. NTAL/LAB is not expressed in normal resting T cells (Brdička et al., 2002) but might be up-regulated in activated T cells (Zhu et al., 2006), and LAB expression can partially restore Ca^{2+} flux in LAT-deficient J.CaM2.5 cells (Janssen et al., 2004). However, we could not detect protein expression in primary T cells of our patient and therefore did not follow up on this protein. Based on the different expression patterns in primary T cells and the J.CaM2.5 cell line, the most potent candidate was CD6, which associates, like LAT, with SLP76 in an activation-dependent manner (Roncagalli et al., 2014). However, in J.CaM2.5 cells and in J.CaM2.5-LAT^{mut} cells, the induced expression of CD6 was not sufficient to elicit Ca^{2+} mobilization upon TCR stimulation. Therefore, it is unlikely that CD6 replaces LAT function in LAT-deficient primary T cells, and the explanation of the preserved Ca^{2+} flux, NF-κB activation in the patient's T cells, and the persistent T cell differentiation remains elusive at this time.

In contrast to Ca^{2+} mobilization, ERK phosphorylation and the up-regulation of CD69 were abolished in primary LAT^{mut}-expressing T cells and in LAT-deficient and LAT^{mut}-expressing J.CaM2.5 cells. A functional Ca^{2+} response but defective ERK signaling in the patient's T cells could be explained by several mechanisms. First, if the LAT-substituting protein allowed TCR-induced activation of PLCγ1, IP_3 and diacylglycerol (DAG) would be produced. IP_3 would cause Ca^{2+} influx, but DAG would not be sufficient to activate ERK. Indeed, using primary human T cells, it was shown that both Ras-activating proteins RasGRP1 (downstream of DAG) and SOS1 are required to activate Ras and thus the ERK pathway after an activating TCR trigger (Poltorak et al., 2014). In fact, LAT tyrosine residues hY171/mY175, hY191/mY195, and hY226/mY235 are indispensable in recruiting Grb2-SOS1 to the membrane activating the ERK pathway (Finco et al., 1998; Zhang et al., 1999a; Sommers et al., 2001; Balagopalan et al., 2010). In this scenario, the LAT-substituting protein would not recruit Grb2. Hence, our finding again corroborates the nonredundant role for hY171/mY175, hY191/mY195, and hY226/mY235 in the activation of ERK (Balagopalan et al., 2010; Poltorak et al., 2014) in humans and mice. Second, IP_3 and DAG would be produced in the patient's T cells, but highly active DAG kinases (DGKs), such as DGKα and DGKζ (Joshi and Koretzky, 2013), would remove DAG so that RasGRP1 could not be activated and, subsequently, Ras would stay inactive. Because we did not find enhanced transcript levels for DGKα and DGKζ in the patient's T cells (unpublished data), we find this possibility less likely.

The observed alteration but not absence of TCR-induced signaling illuminates the phenotype, which resembles more the mouse phenotype of LAT signaling pathology in specific LAT mutations than the severe T cell deficiency in knockout mice. Although first proposed to result from defective positive selection and subsequent expansion of autoreactive T cells (Sommers et al., 2005), Roncagalli et al. (2010) subsequently suggested that hyperactivation of normal T cells triggered by peptide–MHC complexes leads to uncontrolled lymphoproliferation and immune dysregulation. Thus, the clinical presentation of human LAT deficiency resembles previously described immunodeficiencies caused by other alterations in TCR signaling like in ZAP70, ITK, or lymphocyte-specific protein tyrosine kinase (LCK) deficiency, all of which are interaction partners of LAT. Despite the immunological resemblance, especially to LCK deficiency, there are clearly distinct features like the prominent reduction of CD8 T cells in ZAP70 deficiency (Roifman et al., 2010), the absent Ca^{2+} signal in ITK deficiency (Linka et al., 2012), and the preserved ERK signal in LCK deficiency (Hauck et al., 2012) highlighting the complex regulation of the signaling and subsequent effect on T cell differentiation.

Given the severe clinical phenotype and high mortality resulting from the profound combined immunodeficiency and immune dysregulation observed in human LAT deficiency, hematopoietic stem cell transplantation of the index patient was performed. The 1-yr follow-up demonstrated full donor chimerism, resolution of opportunistic infections and autoimmune cytopenias, and disappearance of skin infiltrates without any immunosuppressive treatment. The identification of additional patients with possibly different LAT mutations will shed further light on the full immunological and clinical presentation of human LAT deficiency.

MATERIALS AND METHODS

Patients. The medical records of three siblings, two males and one female, from one Israeli Arab consanguineous kindred were reviewed for data on clinical presentation, immunological features, genetic findings, treatment, and final outcome. All experiments were performed after obtaining parental written informed consent and approval by the Hadassah and Israeli Ministry of Health ethical review boards.

Antibodies used in this study. The following antibodies were used in this study: CD3 AF700, CD4 BV421, CD4 FITC, CD6 APC, CD10 BV605, CD19 APC-Cy7, CD21 PE-Cy7, CD25 PerCP-Cy5.5, CD27 BV421, CD28 PerCP-Cy5.5, CD38 PerCp-Cy5.5, CD45RA APC-Cy7, TCR αβ PerCP-Cy5.5, IL-2 PE, LAT PE, NTAL/LAB APC, and biotin anti–human TCR-Vd2 (BioLegend); TCR-Vd1 APC (Miltenyi Biotec); CD8 APC, CD8 Pacific blue, CD21 PE-Cy7, CD31 PE, CD56 APC, CD69 FITC, CD107a PE, CD127 Alexa Fluor 647, IFN-γ FITC, TCR γδ PE, IgG

Alexa Fluor 700, IκBα PE, ERK1/2(pT202/pY204) AF647, and ZAP70(pY319)/SYK(pY352) APC (BD); IgD FITC and IgA PE (SouthernBiotech); CD3 PE-Cy7, CD4 PE-Cy7, CD8 PE, CD16 FITC, CD45RA FITC, CD45 Pacific blue, Vα24 PE, and Vβ11 FITC (Beckman Coulter); CCR7 PE (R&D Systems); Bruton tyrosine kinase/ITK(pY551/pY511) PE, IL-17 PE, IL-4 APC, and ICOS PE (eBioscience); IgM Alexa Fluor 647 (Jackson ImmunoResearch Laboratories, Inc.); and PLCγ1(pY783) and goat anti–rabbit AF647 (Cell Signaling Technology). For immunohistochemistry, CD21 (Dako), CD20 (Invitrogen), CD3 (Cell Marque), CD4 and CD8 (Spring Bioscience), and Bcl-6 (Leica Biosystems) were used. For immunoblotting LAT (sc-7948; Santa Cruz Biotechnology, Inc.), FLAG tag (AHP1074; AbD Serotec), actin (sc-1616; Santa Cruz Biotechnology, Inc.), PLCγ1 (pY783; no. 2821; Cell Signaling Technology), and ZAP70 (pY319; no. 2701; Cell Signaling Technology) were used.

Whole exome sequencing. Exonic sequences were enriched in the DNA sample of our patient 2 using the SureSelect Human All Exon 50 Mb kit (Agilent Technologies). Sequences were determined by HiSeq2000 (Illumina) as 100-bp paired-end runs. Data analysis including read alignment and variant calling was performed by DNAnexus software using the default parameters with the human genome assembly (hg19; GRCh37) as a reference as previously described (Stepensky et al., 2013). For confirmation of the identified mutation, Sanger sequencing was performed in the index patient, his parents, and two deceased and two living siblings.

Molecular biology. LAT transcript was examined in EBV lines of the index patient and healthy controls. RNA was isolated using the RNeasy Plus Mini kit (QIAGEN), and cDNA was generated by using a Superscript II reverse transcription (Thermo Fisher Scientific). PCR or quantitative PCR using SYBR green I master mix (Roche) was performed with primer pairs spanning exon 1–3 (forward, 5′-TGTTGATGG CACTGTGTGTG-3′; reverse, 5′-TGGGTAGGAGGT GACAGGTG-3′) or full-length LAT covering exon 1–10 (forward, 5′-GTATCCAAGGGGCATCCAGTT-3′; reverse, 5′-CCTCTTCCTCCACTTCCTCTG-3′) and hypoxanthine phosphoribosyltransferase (forward, 5′-TCAGGCAGT ATAATCCAAAGATGGT-3′; reverse, 5′-AGTCTGGCT TATATCCAACACTTCG-3′). Genomic DNA was isolated using the QIAamp DNA Mini kit (QIAGEN). For Sanger sequencing on guide DNA of isolated CD4 CD45R0 T cells, primers in intron 4 (forward, 5′-CTTTCCCTTTTGCAA CTGCT-3′) and intron 5 (reverse, 5′-TTCCCCACACTT ACCACCAT-3′) of *LAT* were designed covering exon 5. For the exclusion of alternative splice variants, primers were designed located in LAT exon 4 (forward, 5′-CTACCCACC TGTCACCTCCTAC-3′), exon 7 (forward, 5′-ATAGTC GTCCTCATCCTCATCC-3′), and exon 10 (reverse, 5′-TTCCTGGGACACATTCACATAC-3′).

RNA sequencing. Cells were sorted from control and patient samples into RLT buffer (QIAGEN). Total RNA was isolated using the RNeasy Micro kit (QIAGEN) according to manufacturer's recommendations. cDNA was generated using an Ovation RNA-Seq system (V2; NuGEN), and libraries were constructed with an Ovation Ultralow system (V2 1–16; NuGEN) according to the manufacturer's instructions. The libraries were subjected to 50 cycles of NextSeq 500 sequencing.

Data analysis was performed with RNAExpress (Illumina), which performed alignment of reads to the human reference genome (hg19; University of California, Santa Cruz) using the STAR aligner and determined differentially expressed genes using DESeq2.

Cloning of FLAG-tagged wild-type and mutant LAT and CD6 and expression in LAT-deficient J.CaM2.5 cells. The human LAT and CD6 cDNAs were provided by the BIOSS Toolbox (human ORFeome V5.1 collection; clones 7273 and 14950; GE Healthcare). Wild-type LAT was amplified from cDNA by a single PCR (forward primer, 5′-TCCGATTGACTG AGTCGCCCGGATCCGCCACCATGGAGGAGGCCA TCCTG-3′; reverse primer, 5′-GGGGGGAGAGGGGCG GAATTCTCATTTGTCGTCGTCGTCTTTGTAGTC GTTCAGCTCCTGCAGATTCTC-3′) and mutant LAT by two consecutive PCRs (both with forward primers as for wild-type LAT; reverse primer for the first PCR, 5′-CCC AAGGGGCTGCG-3′; reverse primer for the second PCR, 5′-GGGGGGAGAGGGGCGGAATTCTCATTTGTC GTCGTCGTCTTTGTAGTCGAATCCCGCCGGGAA GATGGCGTCCGGTGGGAGCCCAAGGGGCTGCG-3′). Both wild-type and mutant LAT amplicons were cloned into BamHI–EcoRI-digested pLVX-S IZ (Dopfer et al., 2014) by the Gibson et al. (2009) assembly method. HEK 293 T cells were transfected with either pLVX-S IZ LAT-FLAG wild type or mutant, together with the packaging plasmids pMD2 vsv.G and pCMV dR8.74. Cell culture supernatants containing lentiviral particles were collected 48 h after transfection and used to infect the LAT-deficient J.CaM2.5 cells. The transduced cells were sorted for the same ZsGreen1 expression. Similarly, CD6 was amplified (forward primer, 5′-CCGGATCTATTTCCGGTGAATTCCTCGAGACTA GTGCCACCATGTGGCTCTTCTTCGGGATC-3′; reverse primer, 5′-AGGGGCGGAATTGGATCCGCGGCC GCCTAGGCTGCGCTGATGTCAT-3′) and cloned into NotI–SpeI-digested pLVX-S IP (Dopfer et al., 2014). Lentiviral particles were produced as described in this paragraph and used to transduce J.CaM2.5, J.CaM2.5-LAT^{mut}, and J.CaM2.5-LAT^{wt} cells. FACS staining revealed transduction efficacy of 40–60% stably expressing CD6. Cultivation in puromycin was used for selection of transduced cells.

Immunoblotting. For the detection of LAT by immunoblotting, J.CaM2.5, J.CaM2.5-LAT^{wt}, or J.CaM2.5-LAT^{mut} cells were lysed, insoluble parts were removed by centrifugation, and the proteins were separated by SDS-PAGE and detected

by immunoblotting according to standard protocols via the C-terminal FLAG tag. To measure phosphorylation of PLCγ1(pY783) and ZAP70(pY319), 10^6 J.CaM2.5, J.CaM2.5-LAT^{wt}, and J.CaM2.5-LAT^{mut} cells were stimulated with 5 µg/ml anti-CD3 (UCHT1) for 3 min at 37°C or left untreated, total cell lysates were separated as before, and protein phosphorylation was detected by immunoblotting using phosphospecific antibodies.

Cell isolation and cultivation. PBMCs were isolated from EDTA blood by Ficoll density gradient centrifugation following standard protocols. CD45R0 CD4 T cells were isolated using a memory $CD4^+$ T cell isolation kit (Miltenyi Biotech) according to the manufacturer's instructions. LAT-deficient J.CaM2.5 cells and primary PBMCs were cultivated in RPMI 1640 (PAN Biotech) containing 10% FCS, 1% penicillin, and 1% streptomycin.

Ca^{2+} mobilization. To analyze Ca^{2+} mobilization, cells were labeled with 4.5 µM Indo-1 and 0.045% Pluronic F-127 (Thermo Fisher Scientific) for 45 min at room temperature. Cells were washed twice, and for primary cells, cell surface staining for CD4, CD8, and CD45RA or additionally TCR γδ was performed for 15 min at room temperature. Ca^{2+} mobilization was determined after incubation with 5 and 0.6 µg/ml anti-CD3 (UCHT1; BD) for 10 min at room temperature. Data acquisition was performed on a cell analyzer (LSR Fortessa; BD). After baseline acquisition for 45 s, cross-linking was performed with 5 µg/ml goat anti–mouse IgG (Jackson ImmunoResearch Laboratories, Inc.). Ionomycin (Sigma-Aldrich) was added as a positive control. J.CaM2.5 cells were stimulated by adding 5 µg/ml anti-CD3 (OKT3) or 5 µg/ml anti-CD3 and preincubated with goat anti–mouse IgG for 30 min at 4°C after a 30-s baseline acquisition. Ca^{2+} flux was recorded for 5 min before ionomycin was added as a loading control.

Signaling assays. For intracellular flow cytometry, cells were incubated with 5 µg/ml anti-CD3 (OKT3) with or without 5 µg/ml anti-CD28 for 30 min on ice. 5 µg/ml goat anti–mouse IgG was added for an additional 30 min. J.CaM2.5 cells were stimulated with 5 µg/ml anti-CD3 (OKT3). For detection of ZAP70(pY319), Bruton tyrosine kinase/ITK(pY551/pY511), PLCγ1(pY783), and ERK1/2(pT202/pY204) cells were stimulated for 2 min with anti-CD3 and for S6(pS235/pS236) and IκBα, for 30 min with anti-CD3/anti-CD28. Immediately after stimulation, cells were fixed and subsequently permeabilized using the Phosflow intracellular staining kit (BD) according to the manufacturer's instructions. Cells were stained with the respective antibodies.

Cytokine production. Intracellular cytokines were determined after stimulation of PBMCs with 10 µg/ml anti-CD3 (OKT3) and 2 µg/ml anti-CD28 (Sanquin) or 5 ng/ml PMA and 0.75 µg/ml ionomycin in the presence of 10 µg/ml brefeldin A (all from Sigma-Aldrich). After 4 h, cells were harvested, and fixation and permeabilization was performed using a staining kit for intracellular cytokines (BD) according to the manufacturer's protocol, and after surface and intracellular staining for 20 min, the cells were analyzed by flow cytometry.

T cell activation and proliferation. For T cell activation, 2×10^5 cells were stimulated with plate-bound anti-CD3 (OKT3) or anti-CD3/anti-CD28 for 16 h at 37°C. Cell lines were stimulated with 5 µg/ml of soluble anti-CD3 (OKT3) for 6–16 h. Subsequently, cells were harvested and stained with the corresponding antibodies. For T cell proliferation, PBMCs were labeled with 0.5 µM CFSE (Thermo Fisher Scientific) according to the manufacturer's instructions. Cells were left untreated or stimulated with 1 µg/ml of plate-bound anti-CD3 or 0.3 µg/ml anti-CD3 and 0.5 µg/ml of soluble anti-CD28 or PHA for 5 d at 37°C. Cells were harvested and stained for CD4 and CD8.

NK cell degranulation. 2×10^5 PBMCs were mixed with 2×10^5 target cells of the human erythroleukemia cell line K562 (American Type Culture Collection) in Iscove's modified Dulbecco's medium (Thermo Fisher Scientific) containing 10% FCS. Cells were spun down for 3 min at 30 *g* and stimulated for 2 h at 37°C. After stimulation, cells were harvested and stained with the corresponding antibodies for flow cytometry to determine CD107 up-regulation on $CD56^+$ $CD3^-$ NK cells, correlating with target cell lysis.

ACKNOWLEDGMENTS

The authors would like to thank Iris Porat, Carmit Lugasy, Ina Stumpf, Liselotte Lenner, the Advanced Diagnostics unit of the Center for Chronic Immunodeficiency, and the BIOSS toolbox for excellent technical assistance. We also thank the team of the Department of Pediatric Hematology Oncology of Ruth Rappaport Children's Hospital for the treatment of the child and the family of the patient for their trust and support. We also thank Burkhart Schraven and Luca Simeoni for discussions.

B. Keller, O.S. Yousefi, S. Unger, W.W. Schamel, and K. Warnatz were supported by the German Federal Ministry of Education and Research (BMBF 01EO1303). P. Stepensky and K. Warnatz received funding from the Deutsche Forschungsgemeinschaft (Discovery and Evaluation of New Combined Immunodeficiency Disease Entities; grant DFG WA 1597/4-1). P. Stepensky was supported by a research grant from the joint fund of the Hebrew University and Hadassah Medical Center. This study was supported in part by the Excellence Initiative of the German Research Foundation (GSC-4, Spemann Graduate School).

The authors declare no competing financial interests.

Submitted: 7 July 2015

Accepted: 4 May 2016

REFERENCES

Abraham, R.T., and A. Weiss. 2004. Jurkat T cells and development of the T-cell receptor signalling paradigm. *Nat. Rev. Immunol.* 4:301–308. http://dx.doi.org/10.1038/nri1330

Aguado, E., S. Richelme, S. Nuñez-Cruz, A. Miazek, A.M. Mura, M. Richelme, X.J. Guo, D. Sainty, H.T. He, B. Malissen, and M. Malissen. 2002. Induction of T helper type 2 immunity by a point mutation in the LAT adaptor. *Science.* 296:2036–2040. http://dx.doi.org/10.1126/science.1069057

Archambaud, C., A. Sansoni, M. Mingueneau, E. Devilard, G. Delsol, B. Malissen, and M. Malissen. 2009. STAT6 deletion converts the Th2 inflammatory pathology afflicting Lat^{Y136F} mice into a lymphoproliferative disorder involving Th1 and CD8 effector T cells. *J. Immunol.* 182:2680–2689. http://dx.doi.org/10.4049/jimmunol.0803257

Balagopalan, L., N.P. Coussens, E. Sherman, L.E. Samelson, and C.L. Sommers. 2010. The LAT story: a tale of cooperativity, coordination, and choreography. *Cold Spring Harb. Perspect. Biol.* 2:a005512. http://dx.doi.org/10.1101/cshperspect.a005512

Brdička, T., M. Imrich, P. Angelisová, N. Brdičková, O. Horváth, J. Špička, I. Hilgert, P. Lusková, P. Dráber, P. Novák, et al. 2002. Non–T cell activation linker (NTAL): a transmembrane adaptor protein involved in immunoreceptor signaling. *J. Exp. Med.* 196:1617–1626. http://dx.doi.org/10.1084/jem.20021405

Brdičková, N., T. Brdička, P. Angelisová, O. Horváth, J. Špička, I. Hilgert, J. Pačes, L. Simeoni, S. Kliche, C. Merten, et al. 2003. LIME: a new membrane Raft-associated adaptor protein involved in CD4 and CD8 coreceptor signaling. *J. Exp. Med.* 198:1453–1462. http://dx.doi.org/10.1084/jem.20031484

Bruyns, E., A. Marie-Cardine, H. Kirchgessner, K. Sagolla, A. Shevchenko, M. Mann, F. Autschbach, A. Bensussan, S. Meuer, and B. Schraven. 1998. T cell receptor (TCR) interacting molecule (TRIM), a novel disulfide-linked dimer associated with the TCR–CD3–ζ complex, recruits intracellular signaling proteins to the plasma membrane. *J. Exp. Med.* 188:561–575. http://dx.doi.org/10.1084/jem.188.3.561

Corse, E., R.A. Gottschalk, and J.P. Allison. 2011. Strength of TCR-peptide/MHC interactions and in vivo T cell responses. *J. Immunol.* 186:5039–5045. http://dx.doi.org/10.4049/jimmunol.1003650

Déchanet, J., P. Merville, A. Lim, C. Retière, V. Pitard, X. Lafarge, S. Michelson, C. Méric, M.M. Hallet, P. Kourilsky, et al. 1999. Implication of γδ T cells in the human immune response to cytomegalovirus. *J. Clin. Invest.* 103:1437–1449. http://dx.doi.org/10.1172/JCI5409

Dopfer, E.P., F.A. Hartl, H.H. Oberg, G.M. Siegers, O.S. Yousefi, S. Kock, G.J. Fiala, B. Garcillán, A. Sandstrom, B. Alarcón, et al. 2014. The CD3 conformational change in the γδ T cell receptor is not triggered by antigens but can be enforced to enhance tumor killing. *Cell Reports.* 7:1704–1715. http://dx.doi.org/10.1016/j.celrep.2014.04.049

Finco, T.S., T. Kadlecek, W. Zhang, L.E. Samelson, and A. Weiss. 1998. LAT is required for TCR-mediated activation of PLCγ1 and the Ras pathway. *Immunity.* 9:617–626. http://dx.doi.org/10.1016/S1074-7613(00)80659-7

Genton, C., Y. Wang, S. Izui, B. Malissen, G. Delsol, G.J. Fournié, M. Malissen, and H. Acha-Orbea. 2006. The Th2 lymphoproliferation developing in Lat^{Y136F} mutant mice triggers polyclonal B cell activation and systemic autoimmunity. *J. Immunol.* 177:2285–2293. http://dx.doi.org/10.4049/jimmunol.177.4.2285

Gibson, D.G., L. Young, R.Y. Chuang, J.C. Venter, C.A. Hutchison III, and H.O. Smith. 2009. Enzymatic assembly of DNA molecules up to several hundred kilobases. *Nat. Methods.* 6:343–345. http://dx.doi.org/10.1038/nmeth.1318

Hauck, F., C. Randriamampita, E. Martin, S. Gerart, N. Lambert, A. Lim, J. Soulier, Z. Maciorowski, F. Touzot, D. Moshous, et al. 2012. Primary T-cell immunodeficiency with immunodysregulation caused by autosomal recessive LCK deficiency. *J. Allergy Clin. Immunol.* 130:1144–1152.e11. http://dx.doi.org/10.1016/j.jaci.2012.07.029

Holst, J., H. Wang, K.D. Eder, C.J. Workman, K.L. Boyd, Z. Baquet, H. Singh, K. Forbes, A. Chruscinski, R. Smeyne, et al. 2008. Scalable signaling mediated by T cell antigen receptor-CD3 ITAMs ensures effective negative selection and prevents autoimmunity. *Nat. Immunol.* 9:658–666. http://dx.doi.org/10.1038/ni.1611

Hur, E.M., M. Son, O.H. Lee, Y.B. Choi, C. Park, H. Lee, and Y. Yun. 2003. LIME, a novel transmembrane adaptor protein, associates with $p56^{lck}$ and mediates T cell activation. *J. Exp. Med.* 198:1463–1473. http://dx.doi.org/10.1084/jem.20030232

Janssen, E., M. Zhu, B. Craven, and W. Zhang. 2004. Linker for activation of B cells: a functional equivalent of a mutant linker for activation of T cells deficient in phospholipase C-γ1 binding. *J. Immunol.* 172:6810–6819. http://dx.doi.org/10.4049/jimmunol.172.11.6810

Joshi, R.P., and G.A. Koretzky. 2013. Diacylglycerol kinases: regulated controllers of T cell activation, function, and development. *Int. J. Mol. Sci.* 14:6649–6673. http://dx.doi.org/10.3390/ijms14046649

Knight, A., A.J. Madrigal, S. Grace, J. Sivakumaran, P. Kottaridis, S. Mackinnon, P.J. Travers, and M.W. Lowdell. 2010. The role of Vδ2-negative γδ T cells during cytomegalovirus reactivation in recipients of allogeneic stem cell transplantation. *Blood.* 116:2164–2172. http://dx.doi.org/10.1182/blood-2010-01-255166

Lin, J., and A. Weiss. 2001. Identification of the minimal tyrosine residues required for linker for activation of T cell function. *J. Biol. Chem.* 276:29588–29595. http://dx.doi.org/10.1074/jbc.M102221200

Linka, R.M., S.L. Risse, K. Bienemann, M. Werner, Y. Linka, F. Krux, C. Synaeve, R. Deenen, S. Ginzel, R. Dvorsky, et al. 2012. Loss-of-function mutations within the IL-2 inducible kinase ITK in patients with EBV-associated lymphoproliferative diseases. *Leukemia.* 26:963–971. http://dx.doi.org/10.1038/leu.2011.371

Malissen, B., C. Grégoire, M. Malissen, and R. Roncagalli. 2014. Integrative biology of T cell activation. *Nat. Immunol.* 15:790–797. http://dx.doi.org/10.1038/ni.2959

Mangan, B.A., M.R. Dunne, V.P. O'Reilly, P.J. Dunne, M.A. Exley, D. O'Shea, E. Scotet, A.E. Hogan, and D.G. Doherty. 2013. Cutting edge: CD1d restriction and Th1/Th2/Th17 cytokine secretion by human Vδ3 T cells. *J. Immunol.* 191:30–34. http://dx.doi.org/10.4049/jimmunol.1300121

Marie-Cardine, A., H. Kirchgessner, E. Bruyns, A. Shevchenko, M. Mann, F. Autschbach, S. Ratnofsky, S. Meuer, and B. Schraven. 1999. SHP2-interacting transmembrane adaptor protein (SIT), a novel disulfide-linked dimer regulating human T cell activation. *J. Exp. Med.* 189:1181–1194. http://dx.doi.org/10.1084/jem.189.8.1181

May, R.M., M. Okumura, C.J. Hsu, H. Bassiri, E. Yang, G. Rak, E.M. Mace, N.H. Philip, W. Zhang, T. Baumgart, et al. 2013. Murine natural killer immunoreceptors use distinct proximal signaling complexes to direct cell function. *Blood.* 121:3135–3146. http://dx.doi.org/10.1182/blood-2012-12-474361

Minegishi, Y., J. Rohrer, E. Coustan-Smith, H.M. Lederman, R. Pappu, D. Campana, A.C. Chan, and M.E. Conley. 1999. An essential role for BLNK in human B cell development. *Science.* 286:1954–1957. http://dx.doi.org/10.1126/science.286.5446.1954

Nuñez-Cruz, S., E. Aguado, S. Richelme, B. Chetaille, A.M. Mura, M. Richelme, L. Pouyet, E. Jouvin-Marche, L. Xerri, B. Malissen, and M. Malissen. 2003. LAT regulates γδ T cell homeostasis and differentiation. *Nat. Immunol.* 4:999–1008. http://dx.doi.org/10.1038/ni977

Okada, R., T. Kondo, F. Matsuki, H. Takata, and M. Takiguchi. 2008. Phenotypic classification of human CD_4^+ T cell subsets and their differentiation. *Int. Immunol.* 20:1189–1199. http://dx.doi.org/10.1093/intimm/dxn075

Ou-Yang, C.W., M. Zhu, D.M. Fuller, S.A. Sullivan, M.I. Chuck, S. Ogden, Q.J. Li, and W. Zhang. 2012. Role of LAT in the granule-mediated cytotoxicity of CD8 T cells. *Mol. Cell. Biol.* 32:2674–2684. http://dx.doi.org/10.1128/MCB.00356-12

Peng, X., Z. Cui, W. Gu, W. Xu, and X. Guo. 2014. Low level of LAT-PLC-γ1 interaction is associated with Th2 polarized differentiation: a contributing factor to the etiology of asthma. *Cell. Immunol.* 290:131–137. http://dx.doi.org/10.1016/j.cellimm.2014.05.012

Poltorak, M., I. Meinert, J.C. Stone, B. Schraven, and L. Simeoni. 2014. Sos1 regulates sustained TCR-mediated Erk activation. *Eur. J. Immunol.* 44:1535–1540. http://dx.doi.org/10.1002/eji.201344046

Roifman, C.M., H. Dadi, R. Somech, A. Nahum, and N. Sharfe. 2010. Characterization of ζ-associated protein, 70 kd (ZAP70)-deficient human lymphocytes. *J. Allergy Clin. Immunol.* 126:1226–33.e1. http://dx.doi.org/10.1016/j.jaci.2010.07.029

Roncagalli, R., M. Mingueneau, C. Grégoire, M. Malissen, and B. Malissen. 2010. LAT signaling pathology: an "autoimmune" condition without T cell self-reactivity. *Trends Immunol.* 31:253–259. http://dx.doi.org/10.1016/j.it.2010.05.001

Roncagalli, R., S. Hauri, F. Fiore, Y. Liang, Z. Chen, A. Sansoni, K. Kanduri, R. Joly, A. Malzac, H. Lähdesmäki, et al. 2014. Quantitative proteomics analysis of signalosome dynamics in primary T cells identifies the surface receptor CD6 as a Lat adaptor-independent TCR signaling hub. *Nat. Immunol.* 15:384–392. http://dx.doi.org/10.1038/ni.2843

Sakaguchi, N., T. Takahashi, H. Hata, T. Nomura, T. Tagami, S. Yamazaki, T. Sakihama, T. Matsutani, I. Negishi, S. Nakatsuru, and S. Sakaguchi. 2003. Altered thymic T-cell selection due to a mutation of the ZAP-70 gene causes autoimmune arthritis in mice. *Nature.* 426:454–460. http://dx.doi.org/10.1038/nature02119

Schatorjé, E.J., E.F. Gemen, G.J. Driessen, J. Leuvenink, R.W. van Hout, and E. de Vries. 2012. Paediatric reference values for the peripheral T cell compartment. *Scand. J. Immunol.* 75:436–444. http://dx.doi.org/10.1111/j.1365-3083.2012.02671.x

Shan, X., and R.L. Wange. 1999. Itk/Emt/Tsk activation in response to CD3 cross-linking in Jurkat T cells requires ZAP-70 and Lat and is independent of membrane recruitment. *J. Biol. Chem.* 274:29323–29330. http://dx.doi.org/10.1074/jbc.274.41.29323

Siggs, O.M., L.A. Miosge, A.L. Yates, E.M. Kucharska, D. Sheahan, T. Brdicka, A. Weiss, A. Liston, and C.C. Goodnow. 2007. Opposing functions of the T cell receptor kinase ZAP-70 in immunity and tolerance differentially titrate in response to nucleotide substitutions. *Immunity.* 27:912–926. http://dx.doi.org/10.1016/j.immuni.2007.11.013

Smith-Garvin, J.E., G.A. Koretzky, and M.S. Jordan. 2009. T cell activation. *Annu. Rev. Immunol.* 27:591–619. http://dx.doi.org/10.1146/annurev.immunol.021908.132706

Sommers, C.L., R.K. Menon, A. Grinberg, W. Zhang, L.E. Samelson, and P.E. Love. 2001. Knock-in mutation of the distal four tyrosines of linker for activation of T cells blocks murine T cell development. *J. Exp. Med.* 194:135–142. http://dx.doi.org/10.1084/jem.194.2.135

Sommers, C.L., C.S. Park, J. Lee, C. Feng, C.L. Fuller, A. Grinberg, J.A. Hildebrand, E. Lacaná, R.K. Menon, E.W. Shores, et al. 2002. A LAT mutation that inhibits T cell development yet induces lymphoproliferation. *Science.* 296:2040–2043. http://dx.doi.org/10.1126/science.1069066

Sommers, C.L., J. Lee, K.L. Steiner, J.M. Gurson, C.L. Depersis, D. El-Khoury, C.L. Fuller, E.W. Shores, P.E. Love, and L.E. Samelson. 2005. Mutation of the phospholipase C-γ1-binding site of LAT affects both positive and negative thymocyte selection. *J. Exp. Med.* 201:1125–1134. http://dx.doi.org/10.1084/jem.20041869

Stepanek, O., P. Draber, and V. Horejsi. 2014. Palmitoylated transmembrane adaptor proteins in leukocyte signaling. *Cell. Signal.* 26:895–902. http://dx.doi.org/10.1016/j.cellsig.2014.01.007

Stepensky, P., A. Saada, M. Cowan, A. Tabib, U. Fischer, Y. Berkun, H. Saleh, N. Simanovsky, A. Kogot-Levin, M. Weintraub, et al. 2013. The Thr224Asn mutation in the VPS45 gene is associated with the congenital neutropenia and primary myelofibrosis of infancy. *Blood.* 121:5078–5087. http://dx.doi.org/10.1182/blood-2012-12-475566

van Gent, R., C.M. van Tilburg, E.E. Nibbelke, S.A. Otto, J.F. Gaiser, P.L. Janssens-Korpela, E.A. Sanders, J.A. Borghans, N.M. Wulffraat, M.B. Bierings, et al. 2009. Refined characterization and reference values of the pediatric T- and B-cell compartments. *Clin. Immunol.* 133:95–107. http://dx.doi.org/10.1016/j.clim.2009.05.020

Villa, A., L.D. Notarangelo, and C.M. Roifman. 2008. Omenn syndrome: inflammation in leaky severe combined immunodeficiency. *J. Allergy Clin. Immunol.* 122:1082–1086. http://dx.doi.org/10.1016/j.jaci.2008.09.037

Xiong, N., and D.H. Raulet. 2007. Development and selection of γδ T cells. *Immunol. Rev.* 215:15–31. http://dx.doi.org/10.1111/j.1600-065X.2006.00478.x

Zhang, W., B.J. Irvin, R.P. Trible, R.T. Abraham, and L.E. Samelson. 1999a. Functional analysis of LAT in TCR-mediated signaling pathways using a LAT-deficient Jurkat cell line. *Int. Immunol.* 11:943–950. http://dx.doi.org/10.1093/intimm/11.6.943

Zhang, W., C.L. Sommers, D.N. Burshtyn, C.C. Stebbins, J.B. DeJarnette, R.P. Trible, A. Grinberg, H.C. Tsay, H.M. Jacobs, C.M. Kessler, et al. 1999b. Essential role of LAT in T cell development. *Immunity.* 10:323–332. http://dx.doi.org/10.1016/S1074-7613(00)80032-1

Zhang, W., R.P. Trible, M. Zhu, S.K. Liu, C.J. McGlade, and L.E. Samelson. 2000. Association of Grb2, Gads, and phospholipase C-γ1 with phosphorylated LAT tyrosine residues. Effect of LAT tyrosine mutations on T cell angigen receptor-mediated signaling. *J. Biol. Chem.* 275:23355–23361. http://dx.doi.org/10.1074/jbc.M000404200

Zhu, M., E. Janssen, K. Leung, and W. Zhang. 2002. Molecular cloning of a novel gene encoding a membrane-associated adaptor protein (LAX) in lymphocyte signaling. *J. Biol. Chem.* 277:46151–46158. http://dx.doi.org/10.1074/jbc.M208946200

Zhu, M., S. Koonpaew, Y. Liu, S. Shen, T. Denning, I. Dzhagalov, I. Rhee, and W. Zhang. 2006. Negative regulation of T cell activation and autoimmunity by the transmembrane adaptor protein LAB. *Immunity.* 25:757–768. http://dx.doi.org/10.1016/j.immuni.2006.08.025